Original article

Nuclear Medicine Communications

Development of neutron-activated samarium-153-loaded polystyrene microspheres as a potential theranostic agent for hepatic radioembolization

Hun Yee Tan[a], Yin How Wong[b], Azahari Kasbollah[c], Mohammad Nazri Md Shah[d], Basri Johan Jeet Abdullah[b,d], Alan Christopher Perkins[e] and Chai Hong Yeong[b]

Purpose **Hepatic radioembolization is an effective minimally invasive treatment for primary and metastatic liver cancers. Yttrium-90 [^{90}Y]-labelled resin or glass beads are typically used as the radioembolic agent for this treatment; however, these are not readily available in many countries. In this study, novel samarium-153 oxide-loaded polystyrene ([^{153}Sm]Sm_2O_3-PS) microspheres were developed as a potential alternative to ^{90}Y microspheres for hepatic radioembolization.**

Methods **The [^{152}Sm]Sm_2O_3-PS microspheres were synthesized using solid-in-oil-in-water solvent evaporation. The microspheres underwent neutron activation using a 1 MW open-pool research reactor to produce radioactive [^{153}Sm]Sm_2O_3-PS microspheres via ^{152}Sm(n,γ)^{153}Sm reaction. Physicochemical characterization, gamma spectroscopy and in-vitro radionuclide retention efficiency were carried out to evaluate the properties and stability of the microspheres before and after neutron activation.**

Results **The [^{153}Sm]Sm_2O_3-PS microspheres achieved specific activity of 5.04 ± 0.52 GBq·g^{-1} after a 6 h neutron activation. Scanning electron microscopy and particle size analysis showed that the microspheres remained spherical with an average diameter of ~33 μm before and after neutron activation. No long half-life radionuclide and elemental impurities were found in the samples. The radionuclide retention efficiencies of the [^{153}Sm]Sm_2O_3-PS microspheres at 550 h were 99.64 ± 0.07 and 98.76 ± 1.10% when tested in saline solution and human blood plasma, respectively.**

Conclusions **A neutron-activated [^{153}Sm]Sm_2O_3-PS microsphere formulation was successfully developed for potential application as a theranostic agent for liver radioembolization. The microspheres achieved suitable physical properties for radioembolization and demonstrated high radionuclide retention efficiency in saline solution and human blood plasma.** ***Nucl Med Commun*** **43: 410–422**

Nuclear Medicine Communications 2022, **43**:410–422

Keywords: hepatic radioembolization, neutron activation, polystyrene microspheres, samarium-153, theranostic

[a]School of Biosciences, Faculty of Health and Medical Sciences, Taylor's University, Selangor, [b]School of Medicine, Faculty of Health and Medical Sciences, Taylor's University, Selangor, [c]Medical Technology Division, Malaysian Nuclear Agency, Selangor, [d]Department of Biomedical Imaging, University of Malaya Medical Centre, Kuala Lumpur, Malaysia and [e]Radiological Sciences, School of Medicine, University of Nottingham, Nottingham, UK

Correspondence to Chai Hong Yeong, PhD, MIPM, School of Medicine, Faculty of Health and Medical Sciences, Taylor's University, 47500 Subang Jaya, Selangor, Malaysia
Tel: +60 16 701 6875; e-mail: chaihong.yeong@taylors.edu.my

Received 22 July 2021 **Accepted** 15 December 2021

Introduction

Liver cancer is the sixth most commonly diagnosed cancer and the fourth leading cause of cancer death worldwide. In 2018, there were an estimated 841 000 new cases and 782 000 deaths due to liver cancer globally [1]. Hepatocellular carcinoma (HCC) accounts for 75–85% cases of primary liver cancer whereas intrahepatic cholangiocarcinoma accounts for 10–15% cases [1]. Chronic infection with hepatitis B or C viruses, heavy alcohol intake, aflatoxin-contaminated foodstuffs, type 2 diabetes, obesity and smoking are the key risk factors for HCC [2]. The mortality rate of HCC is almost equivalent to the incident rate because a majority of the HCC patients are diagnosed at the later stage of liver dysfunction [3].

Several strategies such as surgical resection, liver transplantation and hyperthermia ablation techniques are available for the treatment of liver cancer. For palliative treatment, the available options include transarterial chemoembolization (TACE), transarterial radioembolization (TARE), stereotactic body radiation therapy and systemic chemotherapy [4]. These treatments may prolong patient survival and even improve potential outcomes by shrinking tumours and TARE also offers the potential to downstage lesions allowing subsequent possible liver transplantation or resection [5]. A number of similarities have been reported for TACE and TARE patients; however, treatment with TACE required longer hospitalization compared to TARE [6]. In addition, TARE may be a better option for patients who are not suitable for TACE and it is

0143-3636 DOI: 10.1097/MNM.0000000000001529

also superior to TACE in the context of quality of life [7] and median survival time of more than 3 months [8].

One of the most commonly used radiopharmaceuticals for TARE is yttrium-90 (^{90}Y) microspheres that are commercially available as resin-based SIR-Spheres (Sirtex Medical, New South Wales, Australia) and glass-based TheraSphere (Nordion Inc., Ottawa, Canada) [9]. Studies reported that the mean response rate in HCC patients is between 35 and 47% with a median survival of 15–24 months for TARE [10–13]. Unfortunately, the cost of [^{90}Y]-labelled microspheres is relatively high and it is often a major reason why many eligible patients are withdrawn from this treatment option [14]. Another disadvantage of [^{90}Y]-labelled microspheres is its pure beta (β^-) radiation emission, which makes the personalized internal radiation dosimetry a challenge due to the lack of imaging capability [15,16].

Different radionuclides with suitable imaging and therapy properties such as holmium-166 (^{166}Ho) ($T_{1/2}$ = 26.8 h; $E_{\beta^-(max)}$ = 1854 keV; E_γ = 81 keV), rhenium-188 (^{188}Re) ($T_{1/2}$ = 16.9 h; $E_{\beta^-(max)}$ = 2120 keV; E_γ = 155 keV) and samarium-153 (^{153}Sm) have been explored to be used as a potential alternative to ^{90}Y [17–21]. However, ^{166}Ho and ^{188}Re have relatively short physical half-lives and the production of ^{166}Ho and the ^{188}Re generator requires high neutron flux nuclear reactors that are less available worldwide [22]. In comparison, ^{153}Sm has an optimum half-life of 46.3 h and it emits β^- particles with medium energies of 808 (18%), 705 (50%) and 635 keV (32%), allowing maximum penetration in soft tissue up to 4.0 mm (average 0.8 mm) [17,23]. It also emits gamma (γ) rays of 103 keV (28%) [17] that is well suited for scintigraphy imaging using a gamma camera or single-photon emission computed tomography (SPECT) scanner attached with low energy collimator. In addition, the high thermal neutron activation cross-section (206 barns) of the parent nuclide, ^{152}Sm allows a large quantity of high specific activity ^{153}Sm to be produced via direct neutron capture process, ^{152}Sm(n,γ)^{153}Sm in a nuclear research reactor [17]. There are currently 220 operational research reactors available in over 50 countries according to the International Atomic Energy Agency (IAEA) Research Reactor Database [24].

We hypothesize that [^{153}Sm]-loaded microspheres can be used as an alternative to [^{90}Y]-labelled microspheres for hepatic radioembolization. This study aimed to synthesize samarium-153 oxide-loaded polystyrene ([^{153}Sm]Sm_2O_3-PS) microspheres in the diameter range of 20–60 µm for potential application as a theranostic agent for hepatic radioembolization. The physicochemical properties, as well as radionuclide retention efficiency of the microspheres, were studied.

Materials and methods

Chemicals and materials

Styrene (>99% purity), polyvinyl alcohol (PVA; 99% purity), Sm_2O_3 (99% purity) and chloroform were procured from Sigma-Aldrich (St. Louis, Missouri, USA). The 2,2′-azobis-2-methylpropionitrile (AIBN) was obtained from Fisher Scientific (Hampton, New Hampshire, USA). Toluene (99% purity) and 0.22 µm syringe filter were purchased from Merck (Darmstadt, Germany). All other chemicals used were of analytical grade purity and used without further purification. Deionized water was used in all the experiments unless otherwise stated.

Suspension polymerization synthesis of polystyrene

Polystyrene (PS) used in this study was synthesized from its monomer, styrene, through suspension polymerization in a nitrogen environment. First, 12 g of styrene and 0.12 g of AIBN were added to 175 ml of 1% (w/v) PVA solution in a three-neck flat bottom flask under magnetic stirring at 750 rpm. Then, nitrogen gas purging was performed for 30 min before the heating of the solution mixture to 70 °C. The reaction was continued for 24 h at 70 °C. The synthesized PS was then filtered, washed with distilled water and dried in an oven at 70 °C overnight. The molecular weight of the PS was determined using static light scattering on a BI-MwA molecular weight analyser (Brookhaven Instruments Corporation, Holtsville, New York, USA). The lyophilized PS was dissolved in toluene overnight and filtered through a 0.22 µm nylon filter before being injected into the molecular weight analyser. The average molecular weight (n = 6 batches) was determined and reported as mean ± SD.

Synthesis of [^{152}Sm]Sm_2O_3-PS microspheres

The [^{152}Sm]Sm_2O_3-PS microspheres were synthesized using solid-in-oil-in-water solvent evaporation method. Then, 0.5 g of PS prepared in the earlier process was fully dissolved in 7 ml of chloroform and 0.2 g of [^{152}Sm]Sm_2O_3 was added. The mixture was sonicated for 1 min in an ultrasonic bath before being added dropwise into 200 ml of 4% (w/v) PVA solution. The PVA solution was stirred at 850 rpm with an overhead stirrer (IKA, Wilmington, North Carolina, USA) for at least 12 h for complete solvent evaporation. The resulting [^{152}Sm]Sm_2O_3-PS microspheres were filtered and rinsed with 1.5 M hydrochloric acid (HCl) to remove any free [^{152}Sm]Sm_2O_3. The microspheres were then rinsed with 2 l of distilled water and dried in an oven at 70 °C for 48 h. The dried microspheres were filtered through a 20–60 µm sieve and stored at –20 °C for further analysis.

Neutron activation of [^{152}Sm]Sm_2O_3-PS microspheres

Neutron activation of the [^{152}Sm]Sm_2O_3-PS microspheres was performed in a TRIGA Mark II research reactor (General Atomics, San Diego, California, USA) located at the Malaysian Nuclear Agency, Bangi, Malaysia. Before neutron activation, the [^{152}Sm]Sm_2O_3-PS microspheres were sealed in a polyethylene vial and placed in a polyethylene ampoule [21]. The samples were irradiated using either the pneumatic transfer system (PTS) at a

thermal neutron flux of 5×10^{12} n·cm^{-2}·s^{-1} for 5 min or rotary specimen rack (RR) at a thermal neutron flux of 2×10^{12} n·cm^{-2}·s^{-1} for 6 h.

Radioactivity assays

The activity of the neutron-activated samples was measured using a radiopharmaceutical activity ionization chamber (CRC-127R; Capintec, Florham Park, New Jersey, USA). By using the radioactive decay equation (Equation 1), the physical half-life ($t_{1/2}$) of the [^{153}Sm]Sm_2O_3-PS microspheres was calculated.

$$A = A_o e^{-\lambda t}, \quad (1)$$

where A is activity at the time of measurement, A_o is initial activity, λ is the decay factor = ln $2/t_{1/2}$ and t is the time of measurement. The activity per microsphere (Bq per microsphere) was calculated by dividing the sample activity with the estimated number of microspheres present in the sample.

Determination of radionuclide impurities in neutron-activated [^{153}Sm]Sm_2O_3-PS microspheres

Gamma spectroscopy of the [^{153}Sm]Sm_2O_3-PS microspheres was performed at 24 and 48 h after neutron activation using a coaxial hyperpure germanium detector (Canberra, Meriden, Connecticut, USA). Each sample was counted for 5 min at a calibrated distance. The presence of radionuclide impurities was analysed using gamma spectrum analysis software (Genie 2000 Version 3.2; Canberra).

Characterization of the Sm_2O_3-PS microspheres before and after neutron activation

Scanning electron microscopy and energy-dispersive X-ray spectroscopy

Morphology and chemical composition of the Sm_2O_3-PS microspheres before and after neutron activation were determined using a scanning electron microscope (SEM) and energy-dispersive X-ray (EDX) spectroscopy (Quanta 400; Hillsboro, Oregon, USA), respectively. Samples were mounted on an individual aluminum stub and gold-coated before SEM and EDX scanning.

Microsphere size distribution

A laser scattering-based particle size analyser (Microtrac X100, Honeywell, Montgomeryville, New York, Pennsylvania, USA) was used to measure the average diameter and size distribution of the microspheres before and after neutron activation. The Sm_2O_3-PS microspheres were suspended in distilled water and sonicated before the particle size analysis.

Fourier transform infrared spectrometer

Fourier transform infrared (FTIR) spectrum within 650–4000 cm^{-1} of the PS and Sm_2O_3-PS microspheres before and after neutron activation was analysed using an FTIR spectrometer (Spectrum 100; PerkinElmer Inc., Boston, Massachusetts, USA). Each individual sample was dried overnight at 70 °C before the FTIR spectrum measurement.

Determination of samarium content in [^{152}Sm]Sm_2O_3-PS microspheres

A semiquantitative analysis wavelength-dispersive X-ray fluorescence (WDXRF) spectrometer (Zetium PANanalytical; Malvern PANanalytical Ltd., Malvern, UK) was used to determine the Sm content in the [^{152}Sm]Sm_2O_3-PS microspheres.

Density measurement

The density of the [^{152}Sm]Sm_2O_3-PS microspheres was determined based on Archimedes' principle using a Mettler Toledo density meter (Model ME 204; Mettler Toledo, Columbus, Ohio, USA). Then, the density value was incorporated into Equation (2) to calculate the number of microspheres in any 1 g of samples (particles·g^{-1}) [21].

$$\text{Number of particles per gram} = \frac{6 \times 10^{12}}{\pi \times \rho_s \times D_p^{\,3}}, \quad (2)$$

where D_p is the mean diameter of the microspheres in µm and ρ_s is the density of the microspheres in g·cm^{-3}.

Viscosity measurement

A modular advanced rheometer (HAAKE MARS III; ThermoFisher Scientific Inc., Waltham, Massachusetts, USA) attached with a circulating water bath was used to measure the viscosity, η_o of the [^{152}Sm]Sm_2O_3-PS microspheres suspension in saline solution (2.5% w/v) at 37 °C. Stokes' law was used to study the sedimentation rate (settling velocity) of the suspension (Equation 3) [21].

$$V_{sed} = \frac{g[D_p^2(\rho_s - \rho_f)]}{18 \times \eta_0}, \quad (3)$$

where V_{sed} is the sedimentation rate in cm·s^{-1}, g is the gravitational acceleration constant = 981 cm·s^{-2}, D_p is the mean diameter of the microspheres in cm and η_o is the dynamic viscosity of the fluid in Pascal, P = g·cm^{-1}·s^{-1}.

Differential scanning calorimetry

The differential scanning calorimetry (DSC) analysis of the PS microspheres, Sm_2O_3-PS microspheres and Sm_2O_3 was done using a DSC 8000 system (PerkinElmer Inc.). Each sample of about 5 mg was transferred into an aluminium pan and scanned from 25 to 200 °C at a rate of 10 °C/min. Pyris version 11 software (PerkinElmer Inc.) was used for the analysis.

Thermogravimetric analysis

The thermogravimetric analysis (TGA) profiles of the PS and Sm_2O_3-PS microspheres were obtained using a TGA 8000 system (PerkinElmer Inc.). The TGA profiles of Sm_2O_3 were included for comparison. A sample of ~5 mg was placed on an individual ceramic sample pan and heated from 30 to 800 °C at a rate of 10 °C/min under constant nitrogen flow. The obtained TGA profiles were imported into the Pyris software for analysis.

In-vitro radionuclide retention efficiency

Approximately 100 mg of the neutron-activated [^{153}Sm]Sm_2O_3-PS microspheres were transferred into a polyethylene tube containing 10 ml of saline solution. The tube was rolled on a roller mixer (Movil-Rod; JP Selecta, Barcelona, Spain) at 50 rpm for 1 h at room temperature. Then, the sample was centrifuged at 2000 rpm for 10 min. The activity of the sample was measured using an activity calibrator before 1 ml of the supernatant was transferred into a separate gamma assay vial. The procedure was continued until a total of 8 ml of supernatant was collected over a period of 550 h. The activity of the supernatant was assayed using an automatic gamma counter (2470 Wizard^2; PerkinElmer Inc.). The experiment was then repeated in human blood plasma. Three samples were tested in each experiment. The retention efficiency of the ^{153}Sm in the [^{153}Sm]Sm_2O_3-PS microspheres was calculated using Equation (4) [21].

$$\text{Retention efficiency}(\%) = \frac{(A_{sus} - A_{sup})}{A_{sus}} \times 100\%, \quad (4)$$

where A_{sus} is the activity of [^{153}Sm]Sm_2O_3-PS microspheres suspension before each extraction of 1 ml supernatant and A_{sup} is the activity of 1 ml supernatant.

Results

Synthesis of [^{152}Sm]Sm_2O_3-PS microspheres

The PS microspheres were successfully synthesized using suspension polymerization from styrene monomer with AIBN as the free radical initiator. The suspension polymerization at 70 °C for 24 h produced PS with an average molecular weight of 194.6 ± 12.6 kDa, as determined by a static light-scattering molecular weight analyser. Then, [^{152}Sm]Sm_2O_3-PS microspheres with the addition of 40% (w/w) [^{152}Sm]Sm_2O_3 were successfully synthesized using solid-in-oil-in-water solvent evaporation. The synthesis parameters such as PVA concentration, stirring rate and polymer to solvent ratio were optimized to produce [^{152}Sm]Sm_2O_3-PS microspheres in the diameter range of 20–60 μm.

Neutron activation and radioactivity assays

The neutron-activated [^{153}Sm]Sm_2O_3-PS microspheres achieved a specific activity of 5.04 ± 0.52 GBq·g^{-1} after 24 h of storage (to allow for the radioactive decay of any impurities). The average activity per microsphere was 117.5 Bq. The decay curve of [^{153}Sm]Sm_2O_3-PS microspheres is shown in Fig. 1. The physical half-life of [^{153}Sm]Sm_2O_3-PS microspheres at 46.2 h was found similar to the reported physical half-life of pure ^{153}Sm [17,25–27].

Gamma spectrum of [^{153}Sm]Sm_2O_3-PS microspheres

The gamma spectrum of the [^{153}Sm]Sm_2O_3-PS microspheres showed four photopeaks at 41, 47, 69 and 103 keV (Fig. 2). The two most dominant peaks, 103 and 69 keV, are the principal gamma energies emitted by ^{153}Sm. The other two peaks (41 and 47 keV) are the K-shell characteristic X-rays resulting from the radioactive decay of ^{153}Sm. No radionuclide impurity was observed in the [^{153}Sm]Sm_2O_3-PS microspheres.

Physicochemical properties of the Sm_2O_3-PS microspheres before and after neutron activation

Figure 3 shows the SEM images of the PS and Sm_2O_3-PS microspheres before and after 6 h neutron activation. The microspheres were spherical and smooth. No residual of Sm_2O_3 crystals was observed on the surface of the microspheres (Fig. 3). Neutron irradiation of the [^{152}Sm]Sm_2O_3-PS microspheres for 6 h in the TRIGA Mark II research reactor did not produce any physical damage on the microspheres. The EDX spectra of the PS and Sm_2O_3-PS microspheres before and after neutron activation are given in Fig. 3. Carbon (C) was found on the EDX spectrum of the PS microspheres, which corresponded to the chemical composition of the PS. Due to the limitation of EDX spectroscopy, whereby it could only detect chemical elements with atomic numbers higher than 6, the hydrogen (H) element which should be

Fig. 1

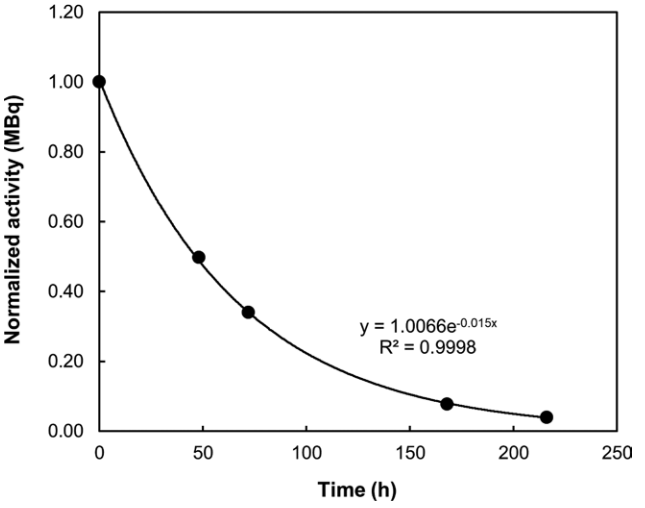

Decay of [^{153}Sm]Sm_2O_3-PS microspheres.

Fig. 2

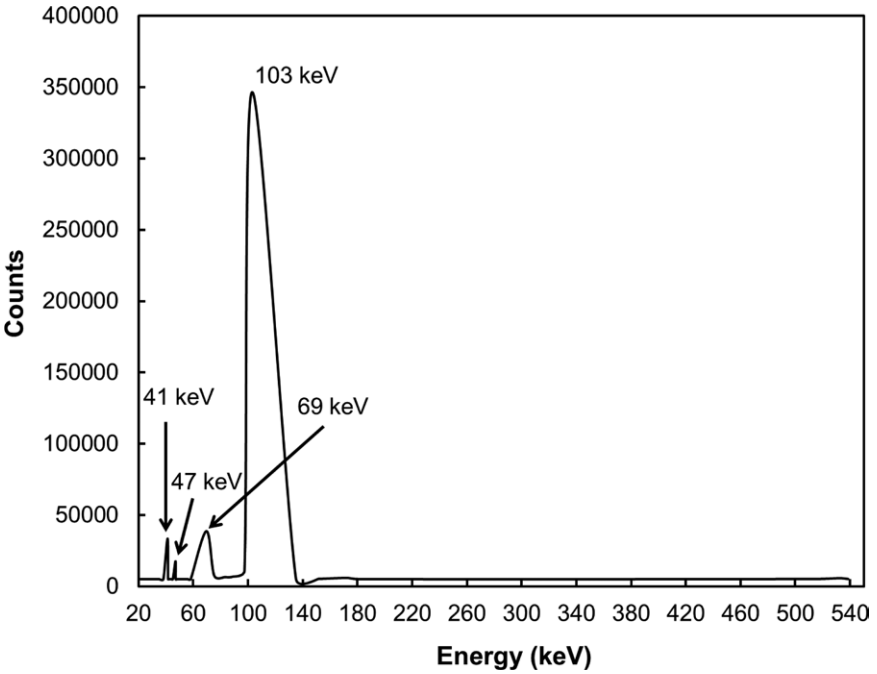

Gamma spectrum of [^{153}Sm]Sm_2O_3-PS microspheres at 24 h after 6 h of neutron activation.

present in PS was not shown in the EDX spectra (Fig. 4a and c). Additional two peaks, which corresponded to Sm and oxygen (O) were found on the EDX spectra of the Sm_2O_3-PS microspheres both before and after neutron activation. Peaks associated with the gold (Au) element were observed in all EDX spectrums. The presence of Au was due to the gold coating of the samples to enhance the conductivity and contrast of the samples. The [^{152}Sm]Sm_2O_3 content in the [^{152}Sm]Sm_2O_3-PS microspheres was 22.44 ± 1.02%, as determined by the WDXRF analysis.

Figure 5 shows the microsphere size distribution of the PS and Sm_2O_3-PS microspheres. The mean diameter of the PS and [^{152}Sm]Sm_2O_3-PS microspheres were 35.63 ± 0.16 and 33.73 ± 0.23 μm, respectively. The mean diameter of the [^{153}Sm]Sm_2O_3-PS microspheres after neutron activation was 33.50 ± 0.18 μm. The size distribution of the PS and Sm_2O_3-PS microspheres both before and after neutron activation were all within the range of 20–60 μm (Fig. 5). Figure 6 shows the FTIR spectra of the PS microspheres, Sm_2O_3-PS microspheres and Sm_2O_3. The FTIR spectrum of the PS microspheres was characterized by the presence of peaks at 3026, 2921, 1602–1452, 753 and 695 cm^{-1}. The occurrence of peaks at 3026 and 2921 cm^{-1} are due to the vibration of aromatic CH and CH_2 groups, respectively. On the contrary, vibrations of aromatic rings produced several peaks within wavelengths of 1602–1452 cm^{-1}. Whereas the peaks at 753 and 695 cm^{-1} could be ascribed to the vibration of the unsubsidized phenyl rings. The FTIR spectra of the Sm_2O_3-PS microspheres before and after neutron activation show similar peaks, with an additional peak at 3600 cm^{-1} as compared to the PS microspheres. The FTIR spectrum of Sm_2O_3 shows a more prominent peak at 3600 cm^{-1}, suggesting that the additional peak in the Sm_2O_3-PS spectra was due to the presence of Sm_2O_3.

The mean density of the PS microspheres was 1.01 ± 0.02 $g{\cdot}cm^{-3}$. The addition of Sm_2O_3 into the PS microspheres increased the density of the Sm_2O_3-PS microspheres to 1.16 ± 0.03 $g{\cdot}cm^{-3}$. The density and mean diameter of the Sm_2O_3-PS microspheres were used to determine the average number of microspheres in 1 g of the sample. There were about 42.9 million microspheres in 1 g of Sm_2O_3-PS microspheres (Table 1). The viscosity profile of the [^{152}Sm]Sm_2O_3-PS microspheres suspension at 37 °C is shown in Fig. 7. The mean viscosity of the [^{152}Sm]Sm_2O_3-PS microspheres suspension was (1.254 ± 0.024) × 10^{-2} $g{\cdot}cm^{-1}{\cdot}s^{-1}$ and the settling velocity was 0.00768 ± 0.00016 $cm{\cdot}s^{-1}$.

The DSC profiles of the PS microspheres, [^{152}Sm]Sm_2O_3-PS microspheres and Sm_2O_3 are presented in Fig. 8. No changes were observed on the DSC curves of all three samples up to 200 °C as the melting point of all three materials is beyond this temperature range. Figure 9 shows the TGA profile of the PS microspheres, [^{152}Sm]Sm_2O_3-PS microspheres and Sm_2O_3. The TGA profile of PS microspheres shows an event of mass

Fig. 3

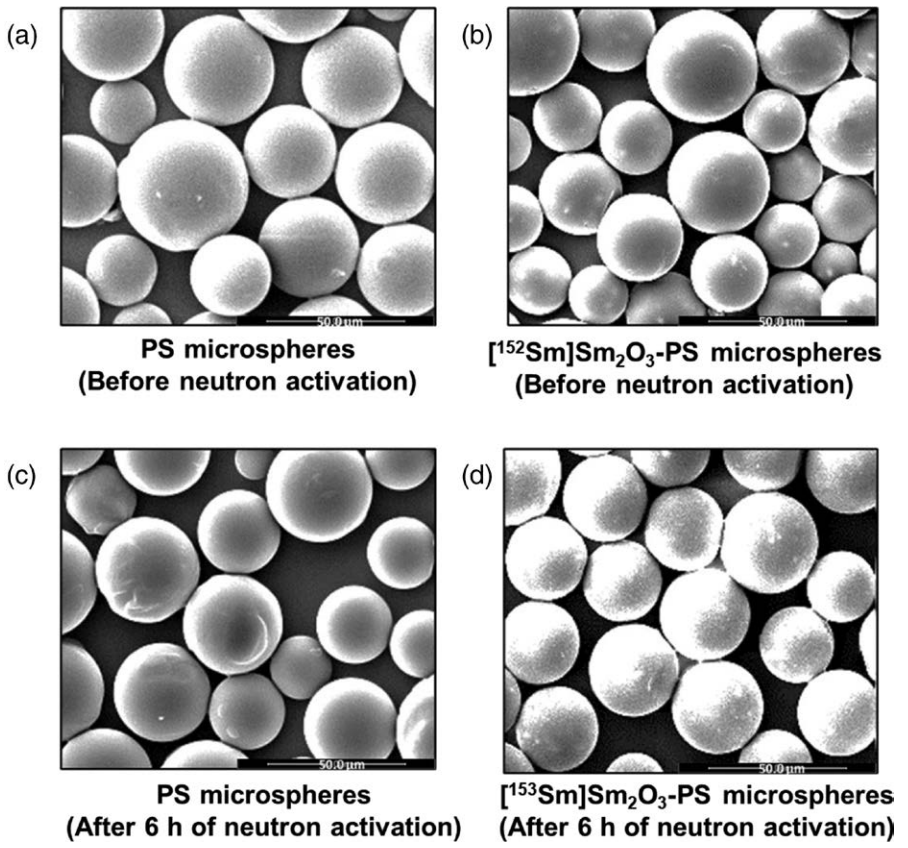

SEM images of PS and Sm_2O_3-PS microspheres both before (a and b) and after (c and d) 6 h of neutron activation. PS, polystyrene; SEM, scanning electron microscopy.

loss starting from 350 °C. The TGA profile of [^{152}Sm]Sm_2O_3-PS microspheres shows the same decomposition step as PS microspheres. The addition of Sm_2O_3 into the PS polymer matrix did not change the decomposition temperature. About 20% residual weight presence in the [^{152}Sm]Sm_2O_3-PS microspheres indicated the presence of Sm_2O_3 in the sample. The TGA profile of Sm_2O_3 did not show any decomposition step up to 100 °C. The content of Sm_2O_3 in the [^{152}Sm]Sm_2O_3-PS microspheres corresponded to the value determined by WDXRF.

In-vitro radionuclide retention efficiency

The [^{153}Sm]Sm_2O_3-PS microspheres demonstrated excellent ^{153}Sm retention efficiencies in both saline solution (99.64 ± 0.07%) and human blood plasma (98.76 ± 1.10%) at 550 h (Fig. 10).

Discussion

We have successfully developed a synthesis workflow for [^{152}Sm]Sm_2O_3 incorporated within biocompatible PS microspheres as a potential theranostic agent for hepatic radioembolization. [^{152}Sm]Sm_2O_3 is a stable chemical that is commercially available from multiple manufacturers. The naturally abundant (26.74%) [^{152}Sm]Sm_2O_3 was used in this study although an enriched form [^{152}Sm]Sm_2O_3 (>98%) is available but with a cost higher by 250–600 times. Because no ionizing radiation is involved during synthesis, this can be carried out in a standard pharmaceutical or chemistry laboratory without concern for radiation protection. The [^{152}Sm]Sm_2O_3-PS microspheres can then be sent for neutron activation to produce radioactive [^{153}Sm]Sm_2O_3-PS microspheres. In this study, a medium thermal neutron flux ($2–5 \times 10^{12}$ n·cm^{-2}·s^{-1}) was used in a TRIGA Mark II nuclear research reactor. Depending on the neutron flux, thermal neutron activation cross-section, mass of the element, atomic weight, isotopic abundance and decay constant, the irradiation time corresponding to the desired activity can be determined. In this study, a 6 h irradiation time was required to achieve a specific activity of 5.04 ± 0.52 GBq·g^{-1} at 24 h after neutron activation. During neutron activation, the ^{152}Sm atoms absorb one neutron from the thermal neutron flux to become radioactive ^{153}Sm, while the extra energy is released as gamma radiation. This reaction is written as ^{152}Sm(n,γ)^{153}Sm.

Detection of long-lived europium radionuclide impurities (especially ^{152}Eu and ^{154}Eu) have been reported in

Fig. 4

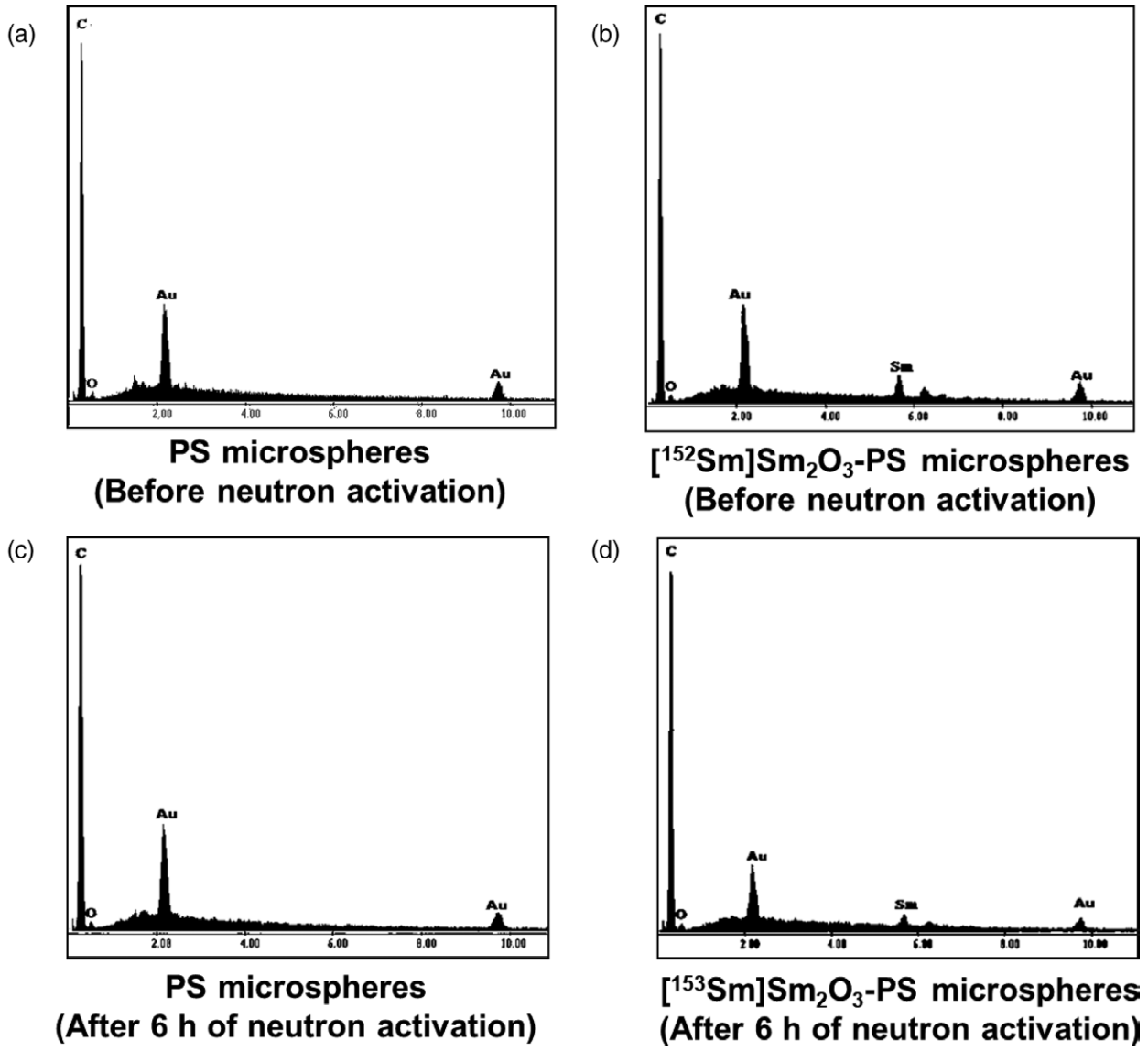

EDX spectra of PS and Sm_2O_3-PS microspheres both before (a and b) and after (c and d) 6 h of neutron activation. EDX, energy-dispersive X-ray; PS, polystyrene.

the commercial [^{153}Sm]-EDTMP product. These radionuclide impurities are produced during the long duration (up to several days) neutron irradiation in the high thermal or epithermal neutron flux when successive neutron capture reactions occur in the daughter isotopes (e.g. one or two neutron capture reactions in ^{153}Eu produce long-lived ^{154}Eu and ^{155}Eu) [28–30]. The impurity levels of [^{153}Sm]-EDMTP depend on various factors, primarily on the elemental and isotopic impurities in target materials, as well as the neutron activation parameters (e.g. thermal and epithermal neutron fluence rates, target shape and size, activation and cooling down times) [29]. Longer irradiation time may produce a higher level of radionuclide impurities due to more successive neutron capture reactions in the daughter isotopes. In the present study, we only employed two neutron irradiation methods and duration, that is, 5 min using the PTS method and 6 h using the RR method. These durations are relatively small compared to the production of commercial [^{153}Sm]-EDTMP formulation. This may explain why no long-lived radionuclide impurities were detected in our samples. However, further research is needed to investigate the radionuclide impurities in our samples associated with longer irradiation time and other neutron activation parameters.

Fig. 5

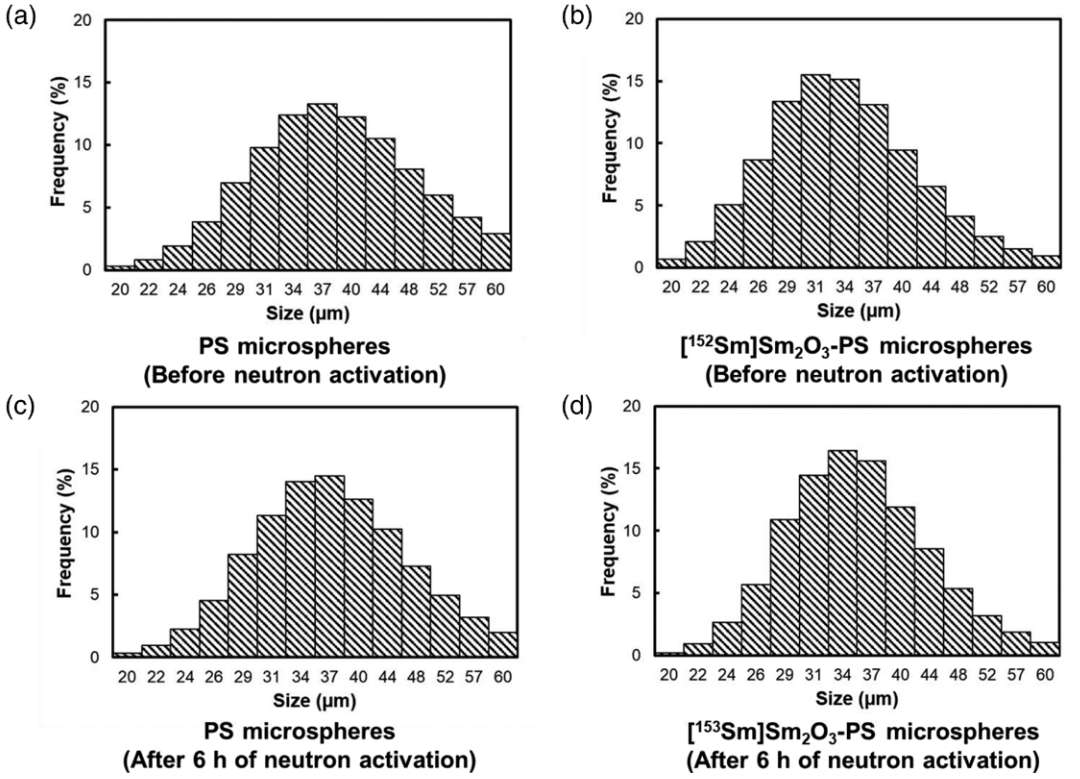

Microsphere size distribution of PS and Sm_2O_3-PS microspheres both before (a and b) and after (c and d) 6 h of neutron activation. PS, polystyrene.

According to the International Pharmacopoeia USP 34, concerning control of radionuclidic purity, not less than 99.8% of total radioactivity must be present as ^{153}Sm at the date of expiration, with ^{154}Eu activity not more than 0.0093% of ^{153}Sm [31]. Various isolation methods for the separation of ^{153}Sm and Eu have been reported in the literature, which include solvent extraction, ion-exchange chromatography, electrochromatography, electrochemical separation and supported ionic liquid phase [32]. This issue needs to be identified and further investigated in the development of [^{153}Sm]Sm_2O_3-PS microspheres for clinical use in the future.

Earlier studies have attempted to develop [^{153}Sm]-labelled microspheres for hepatic radioembolization. Hashikin *et al.* [21] labelled $^{152}Sm^{3+}$ ions to the Amberlite cationic exchange resin through ion exchange reactions. However, the commercially available Amberlite microparticles have a size of ~800 μm. The size of the microparticles was reduced to 20–40 μm by mechanical grinding. The mechanical grinding procedure resulted in the formation of microparticles with an irregular shape, and they were fragmented during the neutron activation procedure, thus resulting in size reduction after neutron activation. On the contrary, Wong *et al.* [33] labelled the commercially available ion-exchange resin microspheres (Toyopearl) readily available in the size of 35 μm diameter with ^{152}Sm chloride hexahydrate ([^{152}Sm]$SmCl_3 \cdot 6H_2O$) and ^{152}Sm carbonate ([^{152}Sm]SmC). Their method produced microspheres that were smooth, spherical and within the desired size of 20–40 μm, both before and after neutron activation. Their study also suggested that [^{152}Sm]SmC-labelled microspheres achieved higher labelling efficiency (97–99%) than ^{153}Sm-labelled microspheres (85–97%). The same research group [20] has also synthesized a new microsphere formulation, poly-L-lactic acid (PLLA) incorporated with ^{152}Sm acetylacetonate ([^{152}Sm]SmAcAc-PLLA). The [^{152}Sm]SmAcAc-PLLA microspheres showed good physiochemical properties as a radioembolic agent except the specific activity was limited at 98 Bq per microsphere due to the maximum loading of [^{152}Sm]SmAcAc on PLLA (175% w/w). In this study, the [^{153}Sm]Sm_2O_3-PS microspheres were developed by encapsulating [^{152}Sm]Sm_2O_3 in the PS microspheres to achieve higher specific activity and radionuclide retention than those produced earlier [20,21,33].

PS is a biocompatible polymer, which has been widely used in several biological and medical applications such as in wound dressings, coating of implantable medical devices and the drug delivery of therapeutic agents [34,35]. The high aromatic hydrocarbon content in PS

Fig. 6

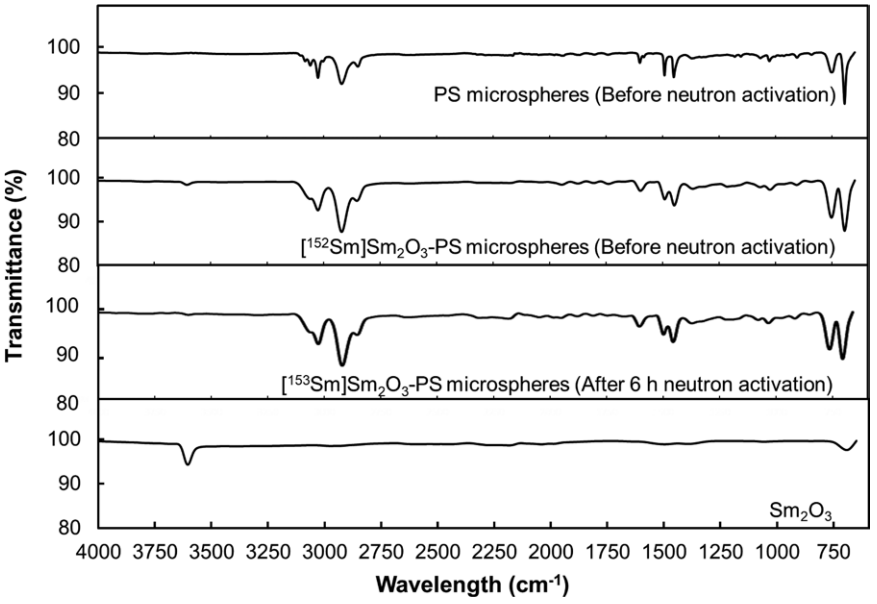

FTIR spectrum of PS microspheres, Sm_2O_3-PS microspheres and Sm_2O_3. FTIR, Fourier transform infrared; PS, polystyrene.

Table 1 Physicochemical characteristics of Sm_2O_3-PS microspheres

Parameters	Sm_2O_3-PS microspheres
Mean size (μm)	33.73 ± 0.23
Density ($g \cdot cm^{-3}$)	1.16 ± 0.03
Viscosity of 2.5% (w/v) microspheres suspension at 37 °C ($\times 10^{-2}$) ($g \cdot cm^{-1} \cdot s^{-1}$)	1.254 ± 0.024
Settling velocity ($cm \cdot s^{-1}$)	0.00768 ± 0.00016
Number of microspheres per gram	42.9 million
Specific activity ($GBq \cdot g^{-1}$)	5.04 ± 0.52
Activity per microsphere (Bq)	117.5

PS, polystyrene.

provides high stability against radiation damage. The electron clouds of aromatic hydrocarbons in PS absorb the radiation and thus prevent the generation of reactive free radicals that could degrade the polymer chain [36]. In addition, PS has a high melting point of about 240 °C [37]; hence, it provides high thermal stability to the [^{152}Sm]Sm_2O_3-PS microspheres. The oxide form of ^{152}Sm ([^{152}Sm]Sm_2O_3) was chosen in this study due to its properties of being poorly soluble in water (and human blood plasma) and being chemically inert so that it can be used safely for intra-arterial administration [37].

One of the critical requirements of a hepatic radioembolic agent is the diameter of the microspheres, which must be in the range of 20–60 μm [38]. This is to ensure that the microspheres will be lodged at the arteriolar network in and around the tumour without crossing over to the venular side through the capillary network (~8–10 μm) [39]. Almost all the synthesis parameters such as polymer concentration, PVA concentration and stirring rate would affect the formation and diameter of the microspheres. These parameters have been optimized in this study to produce spherical microspheres within the size range of 20–60 μm. The unbound Sm_2O_3 and Sm_2O_3 crystals on the surface of the [^{152}Sm]Sm_2O_3-PS microspheres were

Fig. 7

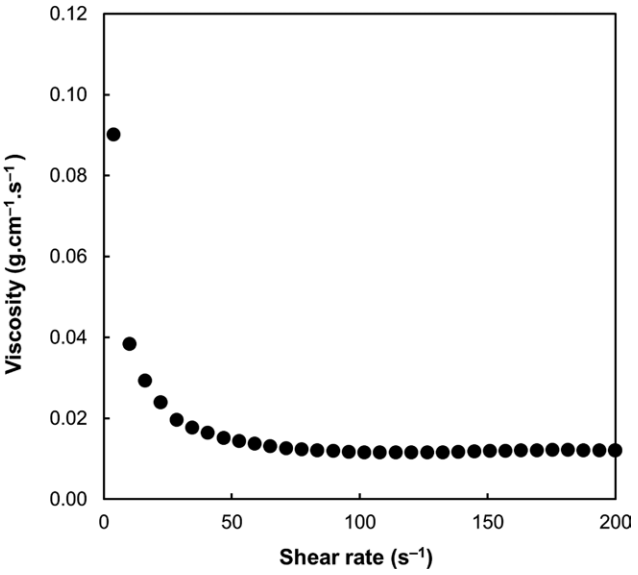

Viscosity of suspension of [^{152}Sm]Sm_2O_3-PS microspheres in saline solution (2.5% w/v) at 37 °C at various shear rates.

Fig. 8

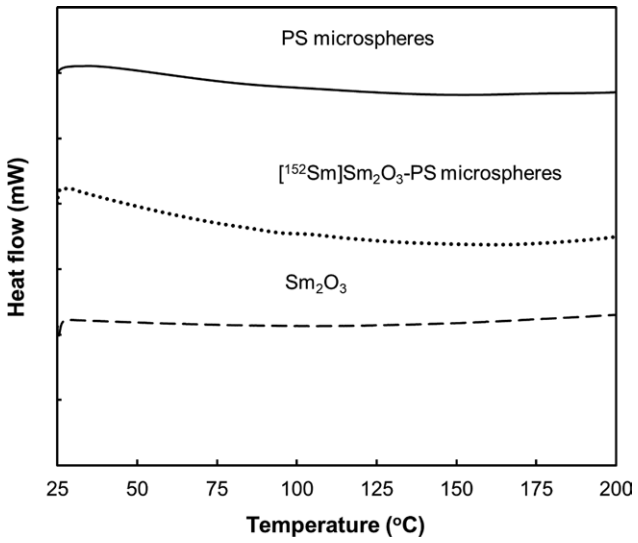

DSC profiles of PS microspheres, [^{152}Sm]Sm_2O_3-PS microspheres and Sm_2O_3. DSC, differential scanning calorimetry; PS, polystyrene.

Fig. 10

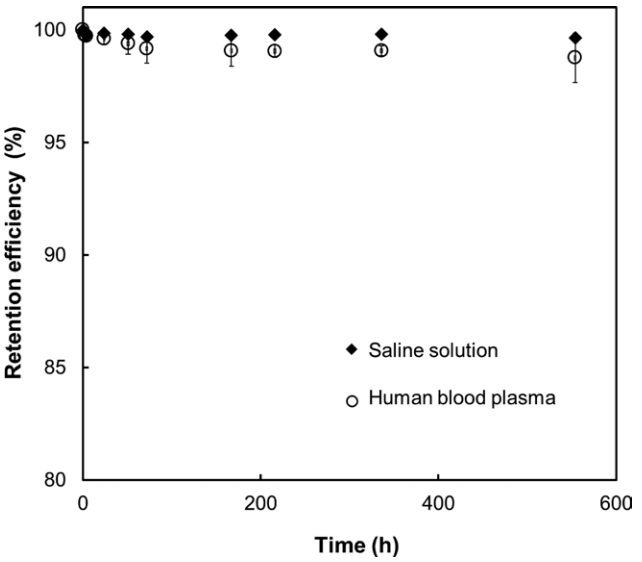

In-vitro retention efficiencies (%) of [^{153}Sm]Sm_2O_3-PS microspheres suspended in saline solution and human blood plasma over 550 h. PS, polystyrene.

Fig. 9

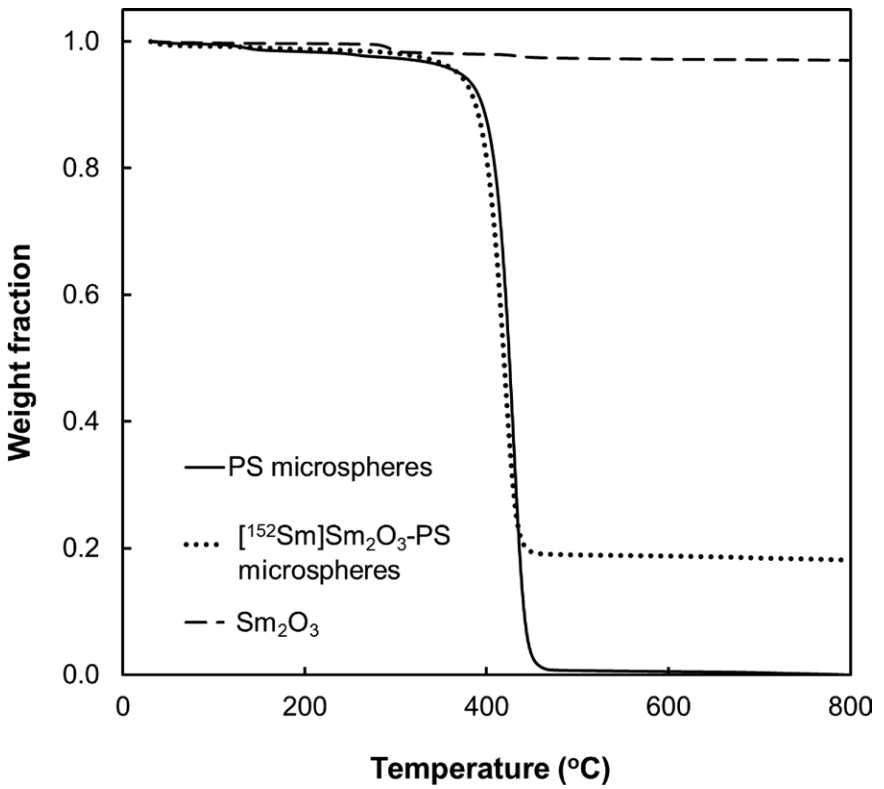

TGA profiles of PS microspheres, [^{152}Sm]Sm_2O_3-PS microspheres and Sm_2O_3. PS, polystyrene; TGA, thermogravimetric analysis.

removed by rinsing with diluted HCl solution. Owing to the high chemical stability of PS, the diluted HCl solution did not cause any physical damage to the [^{152}Sm]Sm_2O_3-PS microspheres. The prolonged neutron irradiation time also did not cause any detrimental effects on the [^{153}Sm]Sm_2O_3-PS microspheres. Unlike those observed with PLLA microspheres [20,40], the [^{152}Sm]Sm_2O_3-PS microspheres did not show any structural fragmentation and size reduction after long hour neutron irradiation. This suggested that the [^{152}Sm]Sm_2O_3-PS microspheres are able to sustain medium thermal neutron flux (in the range of 10^{12} n·cm^{-2}·s^{-1}) and a high-temperature environment in a nuclear reactor. Further studies are needed to evaluate if it could sustain higher levels of thermal neutron flux and temperature.

Because [^{90}Y]-labelled resin or glass microspheres are the only formulations approved by the United States Food and Drug Administration for neoadjuvant treatment of unresectable HCC and liver metastasis from colorectal cancer, the physicochemical properties of the [^{153}Sm]Sm_2O_3-PS microspheres have been compared to the ^{90}Y microspheres (see Table 2). The density of the Sm_2O_3-PS microspheres (1.16 ± 0.03 g·cm^{-3}) is similar to the density of human blood plasma which should enhance the homogeneous distribution of the microspheres within the tumour volume. The [^{153}Sm]Sm_2O_3-PS microspheres have the lowest density compared to [^{90}Y]-labelled resin and glass microspheres and hence it has the lowest sedimentation rate and settling velocity which could prevent the microspheres from settling prematurely in the microcatheter or blood vessel before reaching the tumour volume. In clinical practice, the radioembolic microspheres are administered with saline solution. In view of this, the radionuclide retention efficiency of the [^{153}Sm]Sm_2O_3-PS microspheres was tested in both saline solution and human blood plasma. The retention efficiency of ^{153}Sm in the [^{153}Sm]Sm_2O_3-PS microspheres was excellent (>98%) in both saline solution and human blood plasma over a duration of 550 h. The solid-in-oil-in-water solvent evaporation method has been proven as a convenient and effective method to incorporate [^{152}Sm]Sm_2O_3 into the PS polymer and prevent leaking of the radioactive ^{153}Sm from the microspheres.

Table 2 shows the comparison between [^{153}Sm]Sm_2O_3-PS microspheres developed in this study and commercially available microspheres. Similar to [^{166}Ho]-labelled PLLA microspheres, [^{153}Sm]Sm_2O_3-PS has the advantages of its theranostic properties, can be produced in a nuclear research reactor and decays into a stable daughter. Although ^{166}Ho has higher beta-particle energy and deeper tissue penetration, it has a shorter physical half-life (26.8 h) than ^{153}Sm (46.3 h). Furthermore, thermal neutron activation cross-section of ^{166}Ho is about three times lower than ^{153}Sm (64.7 versus 206 barns); therefore, higher neutron flux or longer irradiation time is required to achieve the desired therapeutic dose. However, due to the low thermal stability of PLLA, the neutron activation time cannot be more than 1 h at a neutron flux of 5×10^{13} cm^{-2}·s^{-1} [32]. According to an earlier publication [42], a total activity of 8.32 GBq from ^{153}Sm is required to achieve a tumour dose of 263 Gy for a liver tumour of 4.3 cm radius (or 333 ml). This is equivalent to 1.82 GBq from ^{90}Y and 5.83 GBq from ^{166}Ho. To achieve this therapeutic dose, 1.65 g of [^{153}Sm]Sm_2O_3-PS is required. Alternatively, the neutron irradiation time may need to be extended, or higher thermal neutron flux may need to be used to increase the specific activity of ^{153}Sm. Further studies are needed to explore these possibilities.

Providing a reactor is available neutron activation is a relatively straight forward and cost-effective method for radionuclide production. In this study, we developed a simple, inexpensive and efficient chemical synthesis workflow for the stable incorporation of (nonradioactive) [^{152}Sm]Sm_2O_3 into PS microspheres. The synthesis can be performed in a standard pharmaceutical or chemical laboratory without concern for radiation exposure. The manufacturer can also consider sterile batch production at their facilities and store the microspheres appropriately before sending for neutron activation. The amount of microspheres to be irradiated (corresponding to product-specific activity) can be determined using the neutron activation formula according to individual treatment plans. In addition, due to the theranostic properties, a low dose of [^{153}Sm]Sm_2O_3-PS can be produced and used for pretreatment dosimetry planning. This would greatly improve the current treatment planning practice in ^{90}Y radioembolization, where a surrogate imaging source, [^{99m}Tc]-macroaggregate albumin (MAA), is used to assess lung shunting and nontarget embolization ratio before ^{90}Y treatment. However, it should be appreciated that [^{99m}Tc]-MAA particles are irregular in size and differ from the shape of [^{90}Y]-microspheres, so they do not fully represent the distribution of the [^{90}Y]-microspheres [38]. The post-administration imaging of ^{90}Y radioembolization also presents a challenge due to the absence of an imaging component. Bremsstrahlung SPECT or PET/computed tomography is often performed after ^{90}Y administration to verify the distribution of the microspheres but both techniques suffer low resolution and low coincidence counts, respectively. With the use of a theranostic agent such as ^{153}Sm and ^{166}Ho, personalized dosimetry can be conveniently achieved to meet the goal of precision medicine. According to the IAEA Research Reactor Database [24], 220 operational research reactors are available globally; therefore, [^{153}Sm]Sm_2O_3-PS can be more widely produced at a lower cost (if it is locally produced) reducing the burden of international radioactive shipping. This would result in lower overall treatment cost and hence more liver cancer patients can be benefited.

Table 2 Comparisons between [^{153}Sm]Sm_2O_3-PS microspheres developed in this study and commercially available radioembolic microspheres

Characteristics	Product name			
	SIR-Spheres [41]	TheraSphere [41]	QuiremSpheres [41]	[^{153}Sm]Sm_2O_3-PS (this study)
FDA approval	Yes	Yes	No	No
Isotope	Yttrium-90 (^{90}Y)		Holmium-166 (^{166}Ho)	Samarium-153 (^{153}Sm)
Half-life (h)	64.1		26.8	46.3
Energy of beta-particles (keV)	2282 (100%)		1854 (50%) 1774 (49%)	808 (18%) 705 (50%) 635 (32%)
Imaging gamma-rays (keV)	No gamma-ray		81 (6%)	103 (28%) 70 (5%)
Tissue penetration (mm)	2.5 (mean) 11 (maximum)		2.5 (mean) 8.4 (maximum)	0.8 (mean) 4.0 (maximum)
Matrix material	Resin	Glass (ceramic)	Poly-L-lactic acid (PLLA)	Polystyrene (PS)
Diameter (μm)	20–60	20–30	15–60	20–60
Density (g·cm^{-3})	1.6	3.3	1.4	1.2
Specific activity per sphere (Bq)	40–70	2500	450	118

Conclusion

Neutron-activated [^{153}Sm]Sm_2O_3-PS microspheres were successfully developed in this study. The nonradioactive [^{152}Sm]Sm_2O_3-PS microspheres were synthesized using a simple solvent evaporation method before neutron activation to produce radioactive [^{153}Sm]Sm_2O_3-PS microspheres. The microspheres achieved specific activity of 5.04 ± 0.52 GBq·g^{-1} after 6 h of neutron activation in a thermal neutron flux of 2×10^{12} n·cm^{-2}·s^{-1}. Neutron activation did not affect the physical and chemical properties of the microspheres. The microspheres remained spherical with diameters within 20–60 μm and had a high in-vitro retention efficiency of more than 98% in saline solution and human blood plasma over 550 h. These formulation properties are desirable for clinical use in liver radioembolization. Further studies are required to assess the cytotoxicity and anticancer efficiency in comparison to ^{90}Y microspheres.

Acknowledgements

The authors would like to acknowledge the supports given by the Malaysian Nuclear Agency and Taylor's University. This study was funded by the Fundamental Research Grant Scheme (FRGS/1/2019/SKK06/TAYLOR/02/3), sanctioned to C.H.Y. by the Ministry of Higher Education, Malaysia. H.Y.T. is scholarly funded by the Taylor's Research Scholarship Programme.

Conflicts of interest

There are no conflicts of interest.

References

1 Bray F, Ferlay J, Soerjomataram I, Siegel RL, Torre LA, Jemal A. Global cancer statistics 2018: GLOBOCAN estimates of incidence and mortality worldwide for 36 cancers in 185 countries. *CA Cancer J Clin* 2018; **68**:394–424.
2 Thun M, Linet MS, Cerhan JR, Haiman CA, Schottenfeld D. *Cancer epidemiology and prevention*. Oxford University Press; 2017.
3 Fattovich G, Stroffolini T, Zagni I, Donato F. Hepatocellular carcinoma in cirrhosis: incidence and risk factors. *Gastroenterology* 2004; **127**:S35–S50.
4 Marrero JA, Kulik LM, Sirlin CB, Zhu AX, Finn RS, Abecassis MM, *et al*. Diagnosis, Staging, and Management of Hepatocellular Carcinoma: 2018 Practice Guidance by the American Association for the Study of Liver Diseases. *Hepatology* 2018; **68**:723–750.
5 Fujiki M, Aucejo F, Choi M, Kim R. Neo-adjuvant therapy for hepatocellular carcinoma before liver transplantation: where do we stand? *World J Gastroenterol* 2014; **20**:5308–5319.
6 Kim HC. Radioembolization for the treatment of hepatocellular carcinoma. *Clin Mol Hepatol* 2017; **23**:109–114.
7 Salem R, Gilbertsen M, Butt Z, Memon K, Vouche M, Hickey R, *et al*. Increased quality of life among hepatocellular carcinoma patients treated with radioembolization, compared with chemoembolization. *Clin Gastroenterol Hepatol* 2013; **11**:1358–1365.e1.
8 Carr BI, Kondragunta V, Buch SC, Branch RA. Therapeutic equivalence in survival for hepatic arterial chemoembolization and yttrium 90 microsphere treatments in unresectable hepatocellular carcinoma: a two-cohort study. *Cancer* 2010; **116**:1305–1314.
9 Lewandowski RJ, Geschwind JF, Liapi E, Salem R. Transcatheter intraarterial therapies: rationale and overview. *Radiology* 2011; **259**:641–657.
10 Lau WY, Ho S, Leung TW, Chan M, Ho R, Johnson PJ, Li AK. Selective internal radiation therapy for nonresectable hepatocellular carcinoma with intraarterial infusion of ^{90}yttrium microspheres. *Int J Radiat Oncol Biol Phys* 1998; **40**:583–592.
11 Geschwind JF, Salem R, Carr BI, Soulen MC, Thurston KG, Goin KA, *et al*. Yttrium-90 microspheres for the treatment of hepatocellular carcinoma. *Gastroenterology* 2004; **127**:S194–S205.
12 Salem R, Lewandowski RJ, Atassi B, Gordon SC, Gates VL, Barakat O, *et al*. Treatment of unresectable hepatocellular carcinoma with use of 90Y microspheres (TheraSphere): safety, tumor response, and survival. *J Vasc Interv Radiol* 2005; **16**:1627–1639.
13 Kulik LM, Atassi B, van Holsbeeck L, Souman T, Lewandowski RJ, Mulcahy MF, *et al*. Yttrium-90 microspheres (TheraSphere) treatment of unresectable hepatocellular carcinoma: downstaging to resection, RFA and bridge to transplantation. *J Surg Oncol* 2006; **94**:572–586.
14 Baum RP. *Therapeutic nuclear medicine*. Springer; 2014.
15 Wright CL, Zhang J, Tweedle MF, Knopp MV, Hall NC. Theranostic Imaging of Yttrium-90. *Biomed Res Int* 2015; **2015**:481279.
16 Kim EE, Lee D, Baum RP, Tateishi U. *Handbook of nuclear medicine and molecular imaging: Principles and clinical applications*. World Scientific Publishing Company; 2012.
17 Pillai M. *Radionuclides for targeted therapy*. Academia; 2007. pp. 50–86.
18 Klaassen NJM, Arntz MJ, Gil Arranja A, Roosen J, Nijsen JFW. The various therapeutic applications of the medical isotope holmium-166: a narrative review. *EJNMMI Radiopharm Chem* 2019; **4**:19.
19 Lepareur N, Lacœuille F, Bouvry C, Hindré F, Garcion E, Chérel M, *et al*. Rhenium-188 labeled radiopharmaceuticals: current clinical applications in oncology and promising perspectives. *Front Med (Lausanne)* 2019; **6**:132.
20 Wong YH, Tan HY, Kasbollah A, Abdullah BJJ, Acharya RU, Yeong CH. Neutron-activated biodegradable samarium-153

acetylacetonate-poly-L-lactic acid microspheres for intraarterial radioembolization of hepatic tumors. *World J Exp Med* 2020; **10**:10–25.
21 Hashikin NA, Yeong CH, Abdullah BJ, Ng KH, Chung LY, Dahalan R, Perkins AC. Neutron activated samarium-153 microparticles for transarterial radioembolization of liver tumour with post-procedure imaging capabilities. *PLoS One* 2015; **10**:e0138106.
22 Knapp F Jr, Beets A, Pinkert J, Kropp J, Lin W, Wang S. *Rhenium radioisotopes for therapeutic radiopharmaceutical development*. IAEA; 2001. pp. 59–66.
23 Lewington VJ. Bone-seeking radionuclides for therapy. *J Nucl Med* 2005; **46**(Suppl 1):38S–47S.
24 IAEA. *Research reactor database*. International Atomic Energy Agency; 2021.
25 Ramamoorthy N, Saraswathy P, Das MK, Mehra KS, Ananthakrishnan M. Production logistics and radionuclidic purity aspects of 153Sm for radionuclide therapy. *Nucl Med Commun* 2002; **23**:83–89.
26 IAEA. *Manual for reactor produced radioisotopes*. International Atomic Energy Agency; 2003.
27 IAEA. *Nuclear data for the production of therapeutic radionuclides*. International Atomic Energy Agency; 2011.
28 Gholipour Peyvandi R, Salehkoutahi M, Shirvani Arani S, Bahrami Samani A, Ghannadi Maragheh M. Assessment of radionuclidic purity of Sm-153 produced by irradiation of natural samarium in Tehran Research Reactor (TRR). *J Nucl Sci Technol* 2009; **30**:6–13.
29 Kalef-Ezra JA, Valakis ST, Pallada S. Samarium-153 EDTMP for metastatic bone pain palliation: the impact of europium impurities. *Phys Med* 2015; **31**:104–107.
30 Van de Voorde M, Van Hecke K, Binnemans K, Cardinaels T. Separation of samarium and europium by solvent extraction with an undiluted quaternary ammonium ionic liquid: towards high-purity medical samarium-153. *RSC Adv* 2018; **8**:20077–86.
31 Nuñez O, Huala R, Pirchio M, Torresi A. Determination of impurities in Sm-153 EDTMP and development of an immediate measurement method. *XLII Annual meeting of the Argentine Association of Nuclear Technology* 2015:1–7.
32 Naseri F, Charkhi A, Salek N, Vosoughi S. The radio-europium impurities in [153Sm]-EDTMP production: a review of isolation methods. *Nucl Med Commun* 2021; **42**:951–963.
33 Wong YH, Tan HY, Kasbollah A, Abdullah BJJ, Yeong CH. Preparation and *In Vitro* evaluation of neutron-activated, theranostic samarium-153-labeled microspheres for transarterial radioembolization of hepatocellular carcinoma and liver metastasis. *Pharmaceutics* 2019; **11**:E596.
34 Dorney J. *Polystyrene: A potential standard for developing in vitro cellular tracking methods for nanotoxicology*. Technological University Dublin; 2013. p. 268.
35 Loos C, Syrovets T, Musyanovych A, Mailänder V, Landfester K, Nienhaus GU, Simmet T. Functionalized polystyrene nanoparticles as a platform for studying bio-nano interactions. *Beilstein J Nanotechnol* 2014; **5**:2403–2412.
36 Sastri V. Chapter 6 – Commodity thermoplastics: polyvinyl chloride, polyolefins, and polystyrene. *Plastics in medical devices*. Elsevier Science; 2014. pp. 73–120.
37 Lynwood C. *Polystyrene: Synthesis, characteristics and applications*. Nova Science Publishers Inc.; 2014.
38 Schulz F, Friebe M. SIRT and its unresolved problems: is imaging the solution? A review. *J Cancer Ther* 2016; **7**:505–18.
39 Kennedy AS, Nutting C, Coldwell D, Gaiser J, Drachenberg C. Pathologic response and microdosimetry of (90)Y microspheres in man: review of four explanted whole livers. *Int J Radiat Oncol Biol Phys* 2004; **60**:1552–1563.
40 Nijsen JF, Zonnenberg BA, Woittiez JR, Rook DW, Swildens-van Woudenberg IA, van Rijk PP, van het Schip AD. Holmium-166 poly lactic acid microspheres applicable for intra-arterial radionuclide therapy of hepatic malignancies: effects of preparation and neutron activation techniques. *Eur J Nucl Med* 1999; **26**:699–704.
41 Pasciak AS, Bradley Y, McKinney JM. *Handbook of radioembolization: Physics, biology, nuclear medicine, and imaging*. CRC Press; 2016.
42 Hashikin NAA, Yeong CH, Guatelli S, Abdullah BJJ, Ng KH, Malaroda A, *et al*. Organ doses from hepatic radioembolization with 90Y, 153Sm, 166Ho and 177Lu: a Monte Carlo simulation study using Geant4. *J Phys Conf Ser* 2016; **694**:012059.